

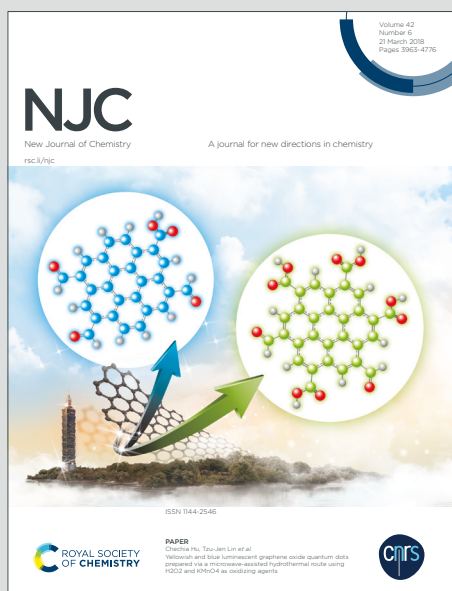
NJC

New Journal of Chemistry

Accepted Manuscript

A journal for new directions in chemistry

This article can be cited before page numbers have been issued, to do this please use: M. fereidoonzhad, H. Ahmadi Mirsadeghi, S. abedanzadeh, A. Yazdani, A. Alamdarlou, M. Babaghasabha, Z. Almansaf, Z. Faghih, Z. McConnell, H. R. Shahsavari and M. H. Beyzavi, *New J. Chem.*, 2019, DOI: 10.1039/C9NJ02502B.



This is an Accepted Manuscript, which has been through the Royal Society of Chemistry peer review process and has been accepted for publication.

Accepted Manuscripts are published online shortly after acceptance, before technical editing, formatting and proof reading. Using this free service, authors can make their results available to the community, in citable form, before we publish the edited article. We will replace this Accepted Manuscript with the edited and formatted Advance Article as soon as it is available.

You can find more information about Accepted Manuscripts in the [Information for Authors](#).

Please note that technical editing may introduce minor changes to the text and/or graphics, which may alter content. The journal's standard [Terms & Conditions](#) and the [Ethical guidelines](#) still apply. In no event shall the Royal Society of Chemistry be held responsible for any errors or omissions in this Accepted Manuscript or any consequences arising from the use of any information it contains.

Synthesis and biological evaluation of thiolate gold(I) complexes as thioredoxin reductases (TrxRs) and glutathione reductase (GR) inhibitors

Masood Fereidoonzhad,^{a,d} Hasti Ahmadi Mirsadeghi,^b Sedigheh Abedanzadeh,^c Alireza Yazdani,^{a,d} Arsalan Alamdarlou,^{a,d} Mojgan Babaghasabha,^b Zainab Almansaf,^e Zeinab Faghieh,^f Zach McConnell,^e Hamid R. Shahsavari,^{*b,e,l} and M. Hassan Beyzavi^{*e}

^aToxicology Research Center; Department of Medicinal Chemistry, School of Pharmacy, Ahvaz Jundishapur University of Medical Sciences, Ahvaz, Iran.

^bDepartment of Chemistry, Institute for Advanced Studies in Basic Sciences (IASBS), Zanjan 45137-66731, Iran.

^cInstitute of Biochemistry and Biophysics (IBB), University of Tehran, Tehran, Iran.

^dStudent Research Committee, Ahvaz Jundishapur University of Medical Sciences, Ahvaz, Iran.

^eDepartment of Chemistry and Biochemistry, University of Arkansas, Fayetteville, Arkansas 72701, United States.

^fPharmaceutical Sciences Research Center, Shiraz University of Medical Sciences, Shiraz, Iran.

^lOn sabbatical leave from IASBS, Zanjan, Iran.

*Email: shahsavari@iasbs.ac.ir, hrshahsa@uark.edu (H.R.S.), beyzavi@uark.edu. (M.H.B.).

Abstract

New gold(I) thiolate complexes [(PPh₂py)Au(SR)], (PPh₂py = 2-(diphenylphosphino)pyridine and SR = deprotonated form of pyridine-2-thiol (HSp₂, **1a**), pyrimidine-2 thiol (HSp₂N, **1b**), benzothiazole-2-thiol (HSbt, **1c**) and 2-thiazoline-2-thiol (HSt, **1d**)) were prepared by the reaction of chloro gold complex [(PPh₂py)AuCl], **A**, with the corresponding *in situ* generated thiolate salt (through a nucleophilic substitution reaction) under inert conditions. All complexes are characterized by NMR spectroscopy and the structures of **1b** and **1d** were further identified by single crystal X-ray determination. An *in vitro* cytotoxicity evaluation against five human cancer cell lines including A549 (nonsmall cell lung cancer), SKOV3 (human ovarian cancer), MCF-7 (human breast cancer), SW1116 (colon cancer) and Hela (cervical cancer) demonstrated the promising antitumor effects of **1b** in comparison with standard auranofin and cisplatin. The effects of these compounds on the proliferation of non-tumoral breast

cell line (MCF-12A) showed good selectivity among tumorigenic and non-tumorigenic cell lines. The results illustrated that **1b** effectively produces cell death by inducing apoptosis in MCF-7 human breast cancer cell line. These complexes inhibit both cytosolic (TrxR1) and mitochondrial (TrxR2) thioredoxin reductases as well as glutathione reductase (GR).

1. Introduction

The chemistry of gold is one of the most remarkable areas in the basic and applied chemistry research. Gold complexes have recently grown increasing attention in the design of new metal-based anticancer drugs in order to overcome the drawbacks of platinum-based chemotherapeutic agents.¹⁻⁵ There have been extensive studies on the therapeutic applications of gold complexes particularly antiproliferative properties against wide range of cancerous cells.⁶⁻⁹ Although, DNA damage is believed to be the dominant mechanism for platinum anticancer agents, later studies have shown that thiol-containing proteins/enzymes, can play important roles in the mechanisms of action of anticancer gold complexes based on the strong binding affinity of gold ions with thiols.¹⁰⁻¹³ Phosphine gold(I) thiolate complexes are promising anticancer agents for *in vitro* and *in vivo* antiproliferative activities.¹⁴⁻²¹ The well-known orally active phosphine Au(I) thiolate complex, auranofin, has exhibited *in vitro* anticancer activities toward human cancer cell lines.²²⁻²⁴ Therefore, a wide investigation has been developed to introduce new phosphine gold(I) thiolate complexes for treatment of various diseases, including several types of leukemia, carcinomas, and parasitic, bacterial, and viral infections.^{6, 25} The nature of ligands in the coordination sphere around the metallic center has essential role to induce specific properties such as stability / reactivity and lipophilicity/hydrophilicity to the metal-based drug. The coordination of thiolate moieties to the gold center has been shown to improve promising *in vitro* and *in vivo* cytotoxic properties of gold complex. In this regard, we designed to prepare a series of structural analogues of 2-(diphenylphosphino)pyridine Au(I) thiolate complexes. 2-(Diphenylphosphino)pyridine, bearing two different hard and soft coordination donor sites, is undoubtedly one of the most attractive family of phosphine compounds which plays an important role in organometallic and coordination chemistry.^{26, 27} It is an unsymmetrical hemilabile ligand that exhibits different physical or chemical properties including luminescence,²⁸⁻³⁰ various coordination modes,^{31, 32} catalytic,³³⁻³⁵ and biological activity.³⁶

Here we present the synthesis, characterization and chemotherapeutic properties of 2-(diphenylphosphino)pyridinegold(I) thiolate complexes of general formula [(PPh₂py)Au(SR)], **1a–d**, SR = deprotonated form of pyridine-2-thiol (HSpy, **1a**), pyrimidine-2 thiol (HSpyN, **1b**), benzothiazole-2-thiol (HSbt, **1c**) and 2-thiazoline-2-thiol (HSt, **1d**), bearing PPh₂py as a P monodentate ligand. The cytotoxic activities of gold(I) complexes have been evaluated against five cancer cell lines, A549, SKOV3, MCF-7, SW1116 and Hela, by means of the MTT assay (MTT= 3-(4,5-dimethylthiazol-yl)-2,5-diphenyl-tetrazolium bromide). The effects of these compounds on the proliferation of non-tumoral cell line (MCF-12A; normal human epithelial breast cell line) was also investigated. Moreover, the ability of **1b** was evaluated to inhibit the proliferation of human breast cancer cells, MCF7, by measuring cell death via induction of apoptosis. *In vitro* inhibition of the complexes on thioredoxin reductase (TrxR) and glutathione reductase (GR) were also acquired.

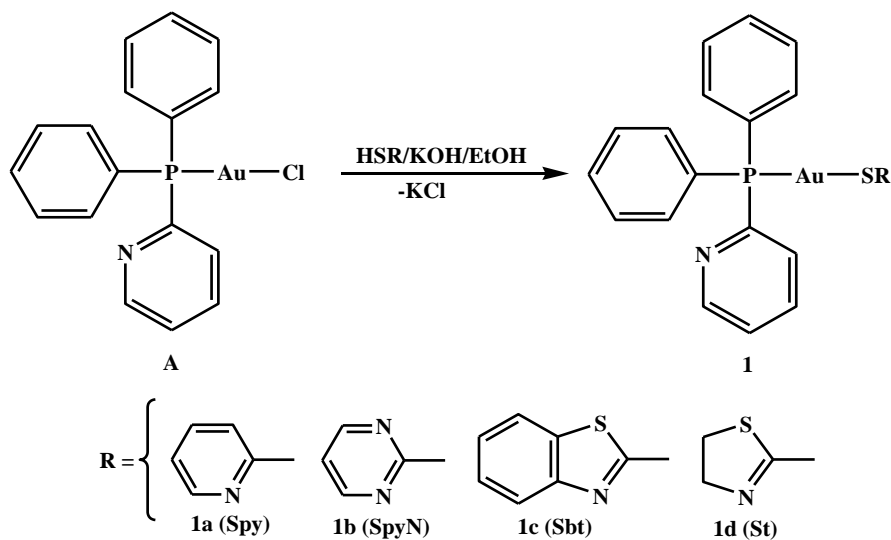
2. Result and Discussion

2.1. Synthesis and characterization of complexes

The known precursor complex [(PPh₂py)AuCl], **A**,³⁷ was synthesized according to the reaction of the PPh₂py ligand (2-(diphenylphosphino)pyridine) with [AuCl(SMe₂)]³⁸ (SMe₂ = dimethylsulfide). Addition of **A** to the corresponding thiolate salt prepared *in situ* by its deprotonation in basic media, lead to produce new gold(I)thiolate complexes[(PPh₂py)Au(SR)], **1a–d**, SR = deprotonated form of pyridine-2-thiol (HSpy, **1a**), pyrimidine-2 thiol (HSpyN, **1b**), benzothiazole-2-thiol (HSbt, **1c**) and 2-thiazoline-2-thiol (HSt, **1d**). General synthetic route is clearly shown in Scheme 1. Eisenberg has also reported **1a**, however, utilizing a different synthetic route.²⁹ All procedures were performed under an argon atmosphere at ambient temperature. In addition, the complexes are well stable at room temperature under the exclusion of light.

All complexes were characterized by NMR spectroscopy. The ¹H and ³¹P{¹H} NMR spectra of each complex show the characteristic resonances of the functional groups present in the molecules while the numerical NMR labeling are shown in Scheme 2. The ¹H NMR and ³¹P{¹H} NMR spectra of **1d** are shown in Figure 1, for clarity. The ³¹P{¹H} NMR spectrum of **A** displays only one singlet resonance at δ = 32.2 ppm corresponding to the P coordinated PPh₂Py moiety which has been shifted to the downfield (36–37 ppm) in new synthesized complexes (**1a–d**). In the ¹H NMR spectra of all five complexes (**A** and **1a–d**), the adjacent proton to the pyridyl moiety

of PPh₂py (H⁶) has been distinguished as a doublet signal located at higher fields (*ca.* 8.80 ppm) with ³J_{HH} values of 4.6 Hz due to the electronic character of nitrogen atom. Aromatic protons were assigned at *ca.* 7–8 ppm, however, protons placed near nitrogen atoms were evidently presented at the higher chemical shifts. In the ¹H NMR spectrum of **1d**, aliphatic protons of 2-thiazoline-2-thiolate ligand (H⁴ and H⁵) appeared with triplet pattern at 3.41 and 4.30 ppm, respectively (Figure 1).



Scheme 1. Synthetic route for the preparation of **1**. All reactions were carried out under an inert gas at room temperature.

Suitable single crystals of **1b** and **1d** were obtained at room temperature by slow diffusion of *n*-hexane into dichloromethane solution of complexes. The ORTEP view, crystal data and structural refinement parameters are determined in Figure 2 and Table 1, respectively. Complexes **1b** and **1d** have been crystallized in the monoclinic space group *P2₁/n*. As shown in Figure 2, each Au(I) center is located in a slightly distorted planar environment, surrounded by phosphorous atom of PPh₂py ligand (P1) and sulphur atom of thiolate moiety (S1). The angles subtended by the ligands at the Au(I) centers (P1-Au1-S1 = 175.53° (8), **1b** and 177.58° (10), **1d**), deviate from the linearity indicating the distorted planar environments. The distance between Au(I) and the thiolate moieties (Au1-S1 = 2.308 Å (2), **1b** and 2.307 Å (2), **1d**) are in accordance with other Au(I) thiolate complexes.^{39, 40}

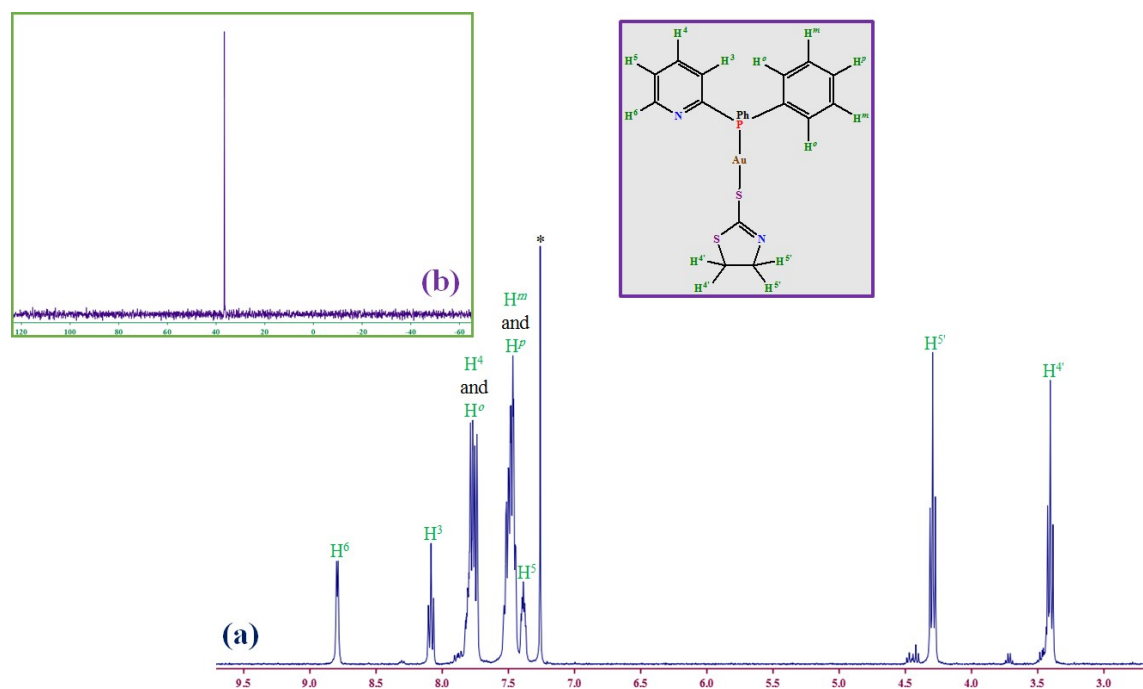


Figure 1. (a) ^1H and (b) $^{31}\text{P}\{^1\text{H}\}$ NMR spectra of **1d** in CDCl_3 at room temperature. The signals assignments are depicted. The NMR solvent residual signal is shown by *.

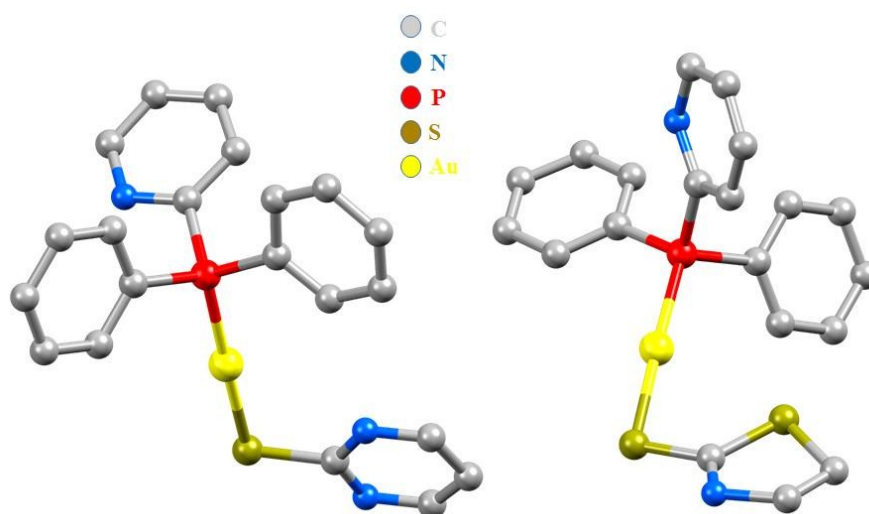


Figure 2. Representations of the X-ray crystal structures of **1b** (left) and **1d** (right) showing all non-hydrogen atoms as 50% thermal ellipsoids. Selected geometrical parameters (\AA , $^\circ$) for **1b**: Au1-P1 2.255(2); Au1-S1 2.308(2); P1-C51.809(7); S1-C11.759(8); P1-Au1-S1 175.53(8); Au1-P1-C5110.9(2); Au1-S1-C1100.6(3). Selected geometrical parameters (\AA , $^\circ$) for **1d**: Au1-P1 2.258(3); Au1-S1 2.307(2); P1-C 71.828(10); S1-C19 1.741(13); P1-Au1-S1 177.58(10); Au1-P1-C7111.7(4); Au1-S1-C19101.8(4).

Table 1. Crystallographic and structure refinement data for **1b** and **1d**.

	1b	1d
Formula	C ₂₁ H ₁₇ AuN ₃ PS	C ₂₀ H ₁₈ AuN ₂ PS ₂
Formula weight	571.38	578.42
T (K)	293(2)	293(2)
λ (Å)	0.71073	0.71073
Crystal system	Monoclinic	Monoclinic
Space group	<i>P</i> 2 ₁ / <i>n</i>	<i>P</i> 2 ₁ / <i>n</i>
Crystal size(mm)	0.12 × 0.22 × 0.22	0.14 × 0.26 × 0.32
<i>a</i> (Å)	9.2477(18)	12.258(3)
<i>b</i> (Å)	17.742(3)	9.6261(19)
<i>c</i> (Å)	12.591(3)	18.107(4)
α (°)	90	90
β (°)	93.63(3)	105.71(3)
γ (°)	90	90
<i>V</i> (Å ³)	2061.7(7)	2056.8(8)
<i>Z</i>	4	4
<i>D</i> _{calc} (g cm ⁻³)	1.841	1.868
θ_{\min} , θ_{\max} (°)	2.654 - 24.998	1.803 - 24.999
<i>F</i> ₀₀₀	1096	1112
μ (mm ⁻¹)	7.325	7.440
Index ranges	-10 ≤ <i>h</i> ≤ 10 -20 ≤ <i>k</i> ≤ 21 -13 ≤ <i>l</i> ≤ 14	-14 ≤ <i>h</i> ≤ 14 -11 ≤ <i>k</i> ≤ 11 -21 ≤ <i>l</i> ≤ 21
Data collected	14486	14476
Unique data	3611	3636
<i>R</i> ₁ ^a , <i>wR</i> ₂ ^b (<i>I</i> > 2 σ (<i>I</i>))	0.0338, 0.0628	0.0462, 0.1026
<i>R</i> ₁ ^a , <i>wR</i> ₂ ^b (all data)	0.0688, 0.0684	0.0820, 0.1147
GOF on <i>F</i> ² (<i>S</i>)	0.882	0.803
CCDC No.	1574994	1574995

$$^a R_1 = \sum ||F_o| - |F_c|| / \sum |F_o|, \quad ^b wR_2 = [\sum (w(F_o^2 - F_c^2)^2) / \sum w(F_o^2)^2]^{1/2}$$

2.2. Biological activity studies

The IC₅₀ of compounds on each cell line is presented in Table 2. Firstly, all of these compounds display good selectivity between tumorigenic and non-tumorigenic cell lines (MCF-12A; normal human epithelial breast cell line). They showed less cytotoxicity than cisplatin and auranofin on MCF-12A. However, one-way ANOVA statistical analysis showed that the differences between **1b** and **1d** with auranofin on MCF-12A is not statistically significant (Table S1-S6). As could be observed, the cytotoxic effect of compounds on cancer cell lines varies from moderate to good effect. The results were compared to cisplatin and auranofin as the reference drugs. All of the synthesized compounds (except **A** and **1d** which is not statistically significant) showed greater anti-proliferative activity than cisplatin, against MCF-7 cell line. In comparison to auranofin, **1b** showed greater and **1c** showed comparable cytotoxic activity on MCF-7 cell line.

One-way ANOVA statistical analysis showed that the differences between **1a**, **1b** and **1c** with auranofin on MCF-7 is not statistically significant. However in the case of SKOV3 cell line, **1a** and **1b** displayed significantly higher *in vitro* cytotoxicity with IC₅₀ of 6.85 and 6.42 μM, respectively, in comparison to cisplatin. This differences is statistically significant. **1a** and **1b** was also showed comparable cytotoxic activity on SKOV3 cell line with auranofin (IC₅₀= 5.28 μM) and these differences is not statistically significant. Regarding A549, **1b** showed comparable cytotoxicity with auranofin as it showed a good anti-proliferative activity with IC₅₀ of 7.67 μM, comparing with that measured for auranofin which was 6.49 μM. However, one-way ANOVA statistical analysis showed that the differences between **1b** and auranofin on A549 is not statistically significant. The cytotoxic activity of the synthesized compounds against Hela cell line was also evaluated. **1b** showed higher anti-proliferative activity than cisplatin and auranofin, however one-way ANOVA statistical analysis showed that the differences between **1b** and auranofin on Hela is not statistically significant. All of the synthesized compounds showed higher cytotoxic activity than cisplatin, against SW1116 cell line. The difference between **1b** with IC₅₀ of 3.31 μM, as the most cytotoxic compound in SW1116 cell line, and auranofin (IC₅₀= 4.20 μM) is not statistically significant.

Structure-activity relationship studies revealed that the presence of non-aromatic ligand (thiolated dihydrothiazole ring in **1d**) decreased cytotoxicity comparing to the other thiolated ligands. Among the aromatic thiolated ligands, **1b** with a thiolated pyrimidine ring showed the highest potency. Complex **A** which encompasses chloro group instead of thiolated ligand showed lowest anti-proliferative activity against all of the studied cell lines.

Table 2. *In vitro* cytotoxic activity against studied tumorigenic and non-tumorigenic cell lines.^a

Complex	(IC ₅₀ ± SD) μM					
	A549	SKOV3	MCF-7	Hela	SW1116	MCF-12A
A	22.08 ± 1.53	16.15 ± 1.74	12.57 ± 0.72	11.21 ± 0.43	15.19 ± 0.61	89.35 ± 1.17
1a	12.71 ± 1.86	6.85 ± 0.26	7.24 ± 0.46	5.19 ± 0.62	7.06 ± 0.33	58.69 ± 1.28
1b	7.67 ± 1.16	6.42 ± 0.27	5.38 ± 0.13	2.29 ± 0.28	3.31 ± 0.52	45.21 ± 2.11
1c	14.48 ± 1.70	14.21 ± 1.08	6.06 ± 0.84	5.17 ± 0.59	9.81 ± 0.25	63.57 ± 1.09
1d	18.09 ± 1.99	14.37 ± 0.42	7.93 ± 1.44	8.51 ± 1.12	12.21 ± 1.60	52.41 ± 2.13

Cisplatin	5.32 ± 0.39	13.29 ± 1.24	10.52 ± 1.39	32.47 ± 1.03	41.69 ± 1.32	32.65 ± 1.22
Auranofin	6.49 ± 0.71	5.28 ± 0.51	6.21 ± 0.89	2.22 ± 0.72	4.20 ± 0.65	49.18 ± 2.32

^a Compounds were dissolved in 1% of DMSO (as described in the Experimental section) and diluted with media before addition to cell culture medium for a 72 hour incubation period. Each experiment was separately repeated three times. Data are presented as mean ± SD.

2.3. Determining apoptotic effect of **1b** on MCF-7 cell line

Using an Annexin V apoptosis detection kit, we evaluated the apoptotic effect of **1b** on MCF-7 cell line. As a normal process, apoptosis or programmed cell death plays a crucial role in tissue homeostasis. Loss of plasma membrane asymmetry is one of the morphologic features happened during the early steps of apoptosis. In apoptotic cells, phosphatidylserine (PS) which is normally found on the inner layer of the plasma membrane translocates to the external leaflet. It thereby can be specifically recognized by a fluorochrome-labeled Annexin V which is a sensitive probe with high affinity for PS. 7-AAD (7-Aminoactinomycin D), a DNA binding reagent was also used to discriminate live healthy cells from dead cells (necrotic or late-apoptotic cells) through penetrating into the nucleus of damaged cells. To determine the apoptotic effect of **1b**, MCF-7 cells were treated with 3 different concentrations of this compound (2.5, 5 and 10 μM). As could be observed in Figure 3, the percentage of the Annexin V+ cells which entered in early apoptotic phase (right side), remarkably increased from 10.8% in untreated cells to 33.3%, 72.6% and 76.5% in the cells following treatment with 2.5, 5 and 10 μM of **1b** for 48 h, respectively. These results indicated that this compound could obviously induce apoptosis in cancerous cells in a dose dependent manner. As shown in Figure 3, after a 48-hour treatment with **1b**, most cells were undergoing apoptosis (Annexin V positive and 7-AAD negative). A minor population of them were observed to be positive for both Annexin V and 7-AAD, which indicates that that they were in the end stage of apoptosis or already dead.

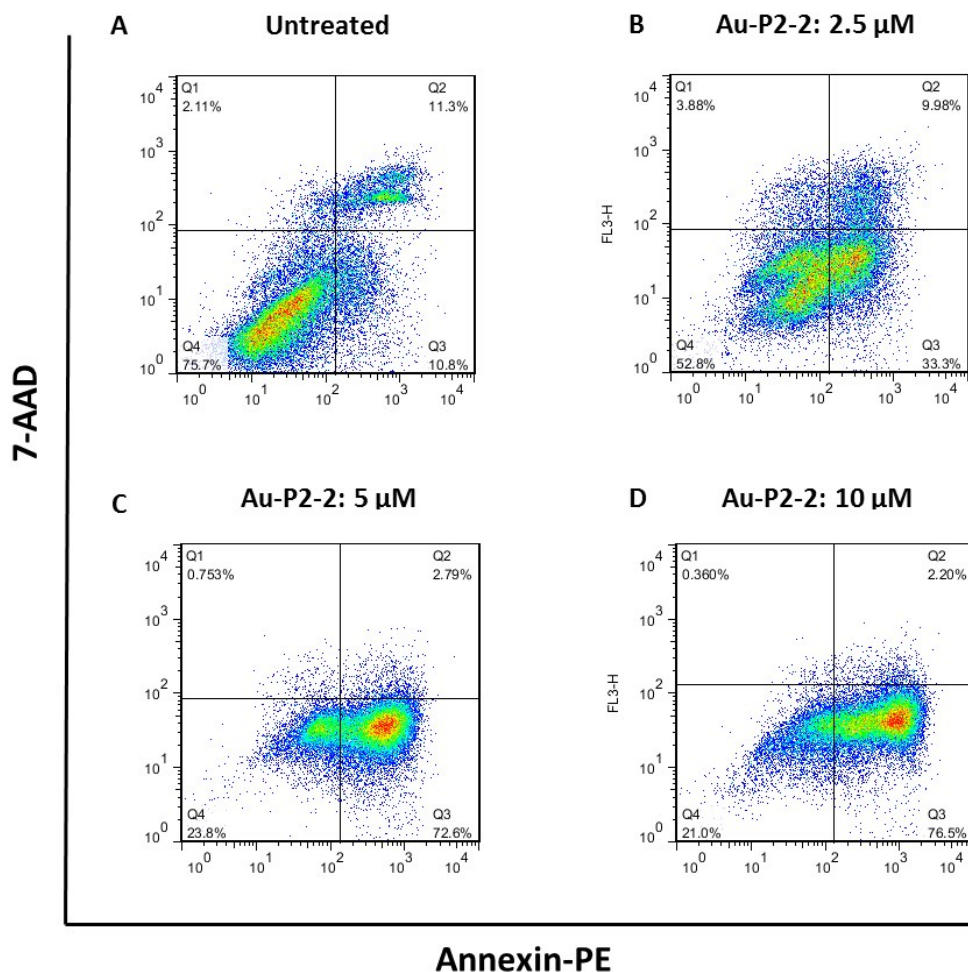


Figure 3. Flow cytometric analysis of apoptotic effect of **1b**. MCF-7 cells (Human breast carcinoma) were left untreated (A) or treated for 48 h with 2.5, 5 and 10 μ M of **1b** (B, C and D). Untreated cells (A) were mostly negative for both Annexin V and 7-AAD and therefore are viable.

2.4. *In vitro* inhibition of thioredoxin reductase (TrxR) and glutathione reductase (GR)

Compounds **A** and **1a-d** were *in vitro* tested for their ability to inhibit both cytosolic (TrxR1) and mitochondrial (TrxR2) thioredoxin reductases as well as glutathione reductase (GR). The results are compared with the reference drug, auranofin, as the potent inhibitor of TrxR enzymes that it has been shown *in vitro* and *in vivo* to have anticancer potential.

As shown in Figure 4, the gold(I) complexes (**A** and **1a-d**) at 20 μ M are potent inhibitors of TrxR1, like cisplatin, and auranofin (at 1 μ M), but testing of enzyme inhibition assay at lower concentrations showed that the synthesized compounds slightly less evident inhibitors of TrxR2

and, interestingly, also inhibit GR while cisplatin or auranofin (at 1 μM) is not inhibiting GR. The dual TrxR1 + GR inhibition is interesting from a mechanistic stand point. GR is usually quite sturdy against inhibitors of TrxR1, although we have seen similar effects with e.g. "TRi-55" in Arnér *et al.* work.⁴¹

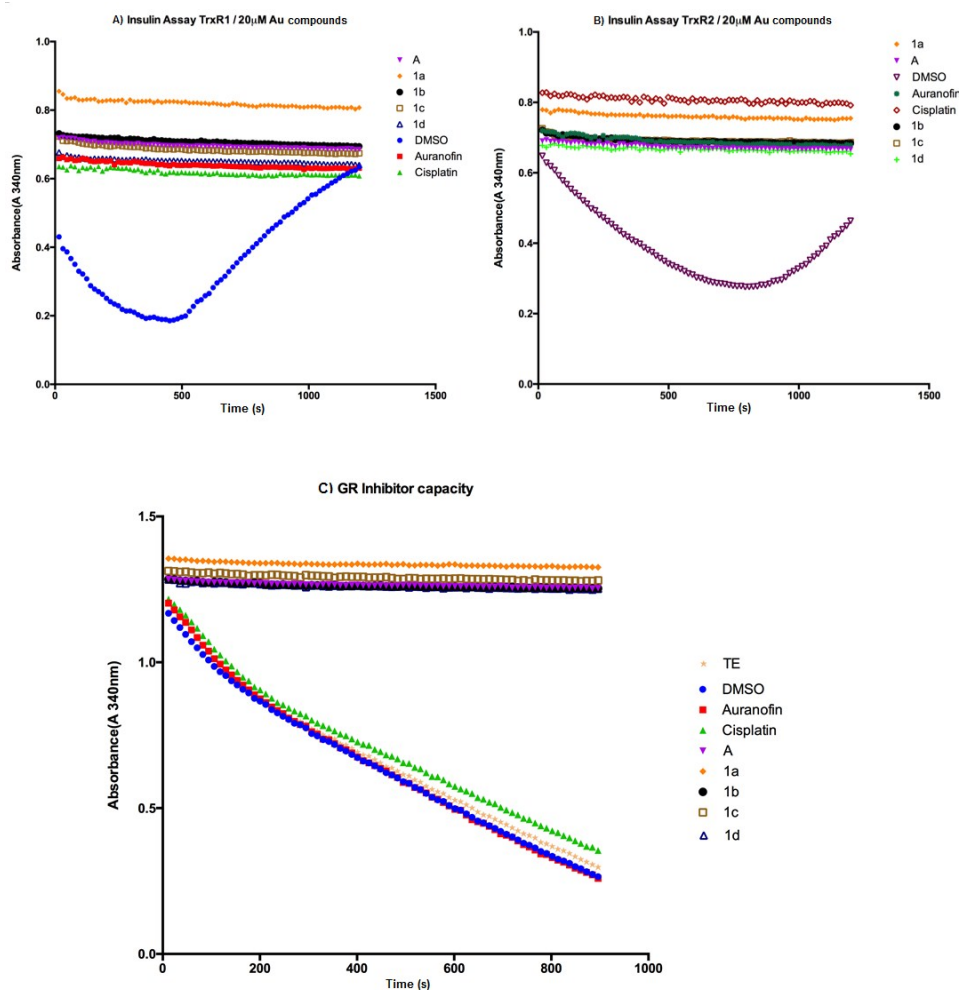


Figure 4. The inhibitor capacity of complexes **A**, **1a-d** on TrxR1, TrxR2 and Gr. The gold(I) complexes (**A** and **1a-d**) at 20 μM are potent inhibitors of TrxR1 and TrxR2, like cisplatin, and auranofin (at 1 μM). They also inhibit GR while cisplatin or auranofin (at 1 μM) is not inhibiting GR.

Using additional concentrations (0.125 μM , 0.25 μM , 0.5 μM , 1 μM , 2 μM and 4 μM), the second order rate constants in inhibition of compounds on TrxR1 and GR were determined. As it was clear in Figure 5, a time delay in enzyme activity initiation after incubation with some of the compounds, which it can be suggested is due to a slow non-specific binding of the compounds to

bovine serum albumin (BSA) that eventually "relieves" the reductase from non-irreversible inhibition, while the irreversible inhibition, of course, cannot be altered (as reflected by the slope in activity one it has started).

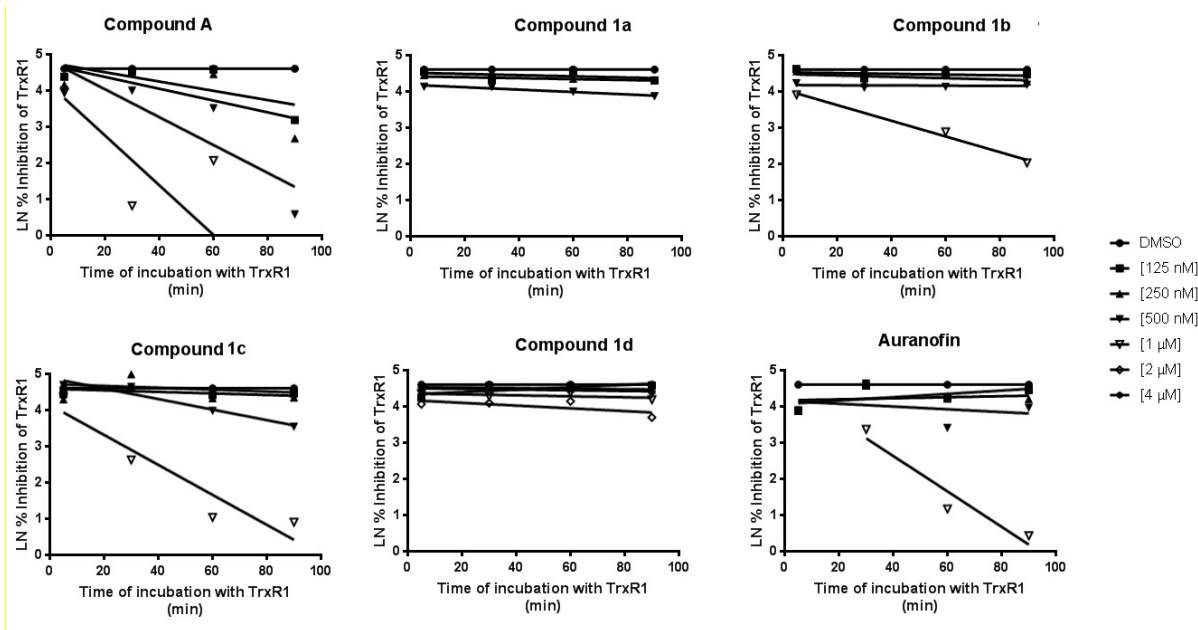


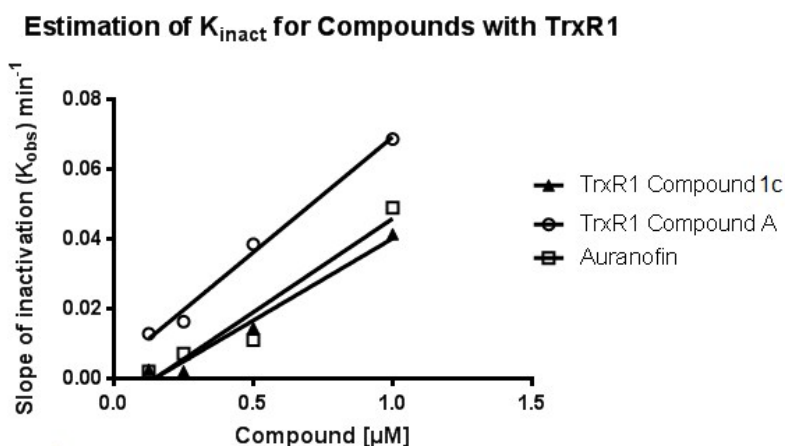
Figure 5. % Inhibition of complexes **A**, **1a-d** and auranofin against time of incubation with TrxR1.

The percentage of inactivation compared to DMSO control was plotted against time using GraphPad Prism 5.0a (GraphPad software, Inc.). The resulting slopes (k_{obs}), were plotted against the inhibitor concentrations resulting in K_{inact} (the rate of enzyme inactivation). The K_{inact} for complexes **A**, **1c** and auranofin with TrxR1 were calculated in Figure 6. The K_{inact} of **A** and **1b** is greater than what it was measured for **1c** and auranofin. It seemed, **A** is a good inhibitor of TrxR1 and more potent than auranofin. However one-way ANOVA statistical analysis showed that, this differences between K_{inact} of **1b** and **1c** with auranofin is not statistically significant.

In addition, the inhibitory activity of complexes towards disulfide reductase GR has been acquired. Figure 7 shows that, **1c** revealed a significant ability of inhibiting GR similar to that observed for auranofin. The rate of enzyme inactivation of **1c** is greater than what it was calculated for auranofin. Hence, **1c** is a good inhibitor of GR.

3. Conclusion

The synthesis of new 2-(diphenylphosphino)pyridine gold(I) complexes with various heterocyclic thiolate ligands with good yields is reported. All of the new complexes were characterized by NMR spectroscopy. The molecular and crystal structures of new compounds **1b** and **1d** were determined by single crystal X-ray crystallography. Treatment of new synthesized gold(I) thiolate complexes on five cancer cell lines, A549, SKOV3, MCF-7, SW1116 and Hela demonstrated considerable cytotoxic activities. The effects of these compounds on the proliferation of non-tumoral cell line (MCF-12A) showed good selectivity between tumorigenic and non-tumorigenic cell lines. According to the results, **1b** showed the highest potential cytotoxic activity among the complexes and significantly exhibited higher *in vitro* cytotoxicity than *cisplatin* against MCF-7 cells lines. Moreover, **1b**, as the most effective compound, has indicated apoptosis-inducing activities to MCF-7 cancer cell line in a dose dependent manner. These complexes were a potent inhibitor of thioredoxin reductases (TrxR) and glutathione reductase (GR). Thiolate ligands confer higher stability under physiological conditions, which leads to an enhancement of their effectiveness as cytotoxic derivatives. Based on this study, **1b** can be introduced as an efficient anticancer agent for further *in vitro* and *in vivo* biological studies in order to develop the non-platinum chemotherapeutic metallopharmaceuticals.



$$\text{Compound 1c: } K_{inact} = 0.047 \pm 0.0054 \mu\text{M}^{-1} \text{ min}^{-1}$$

$$\text{Compound A: } K_{inact} = 0.066 \pm 0.0046 \mu\text{M}^{-1} \text{ min}^{-1}$$

$$\text{Auranofin: } K_{inact} = 0.054 \pm 0.0098 \mu\text{M}^{-1} \text{ min}^{-1}$$

Figure 6. Estimation of the rate of enzyme inactivation (K_{inact}) for **A**, **1c** and auranofin with TrxR1.

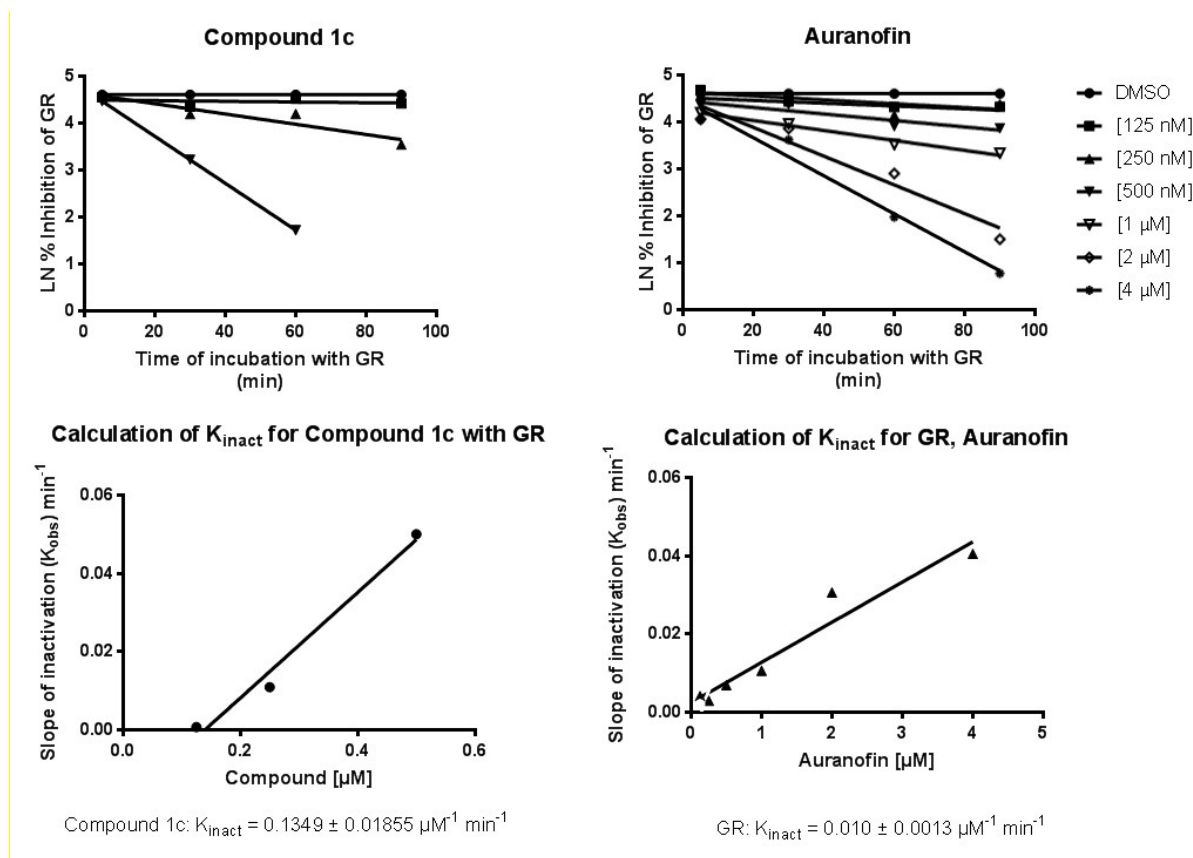


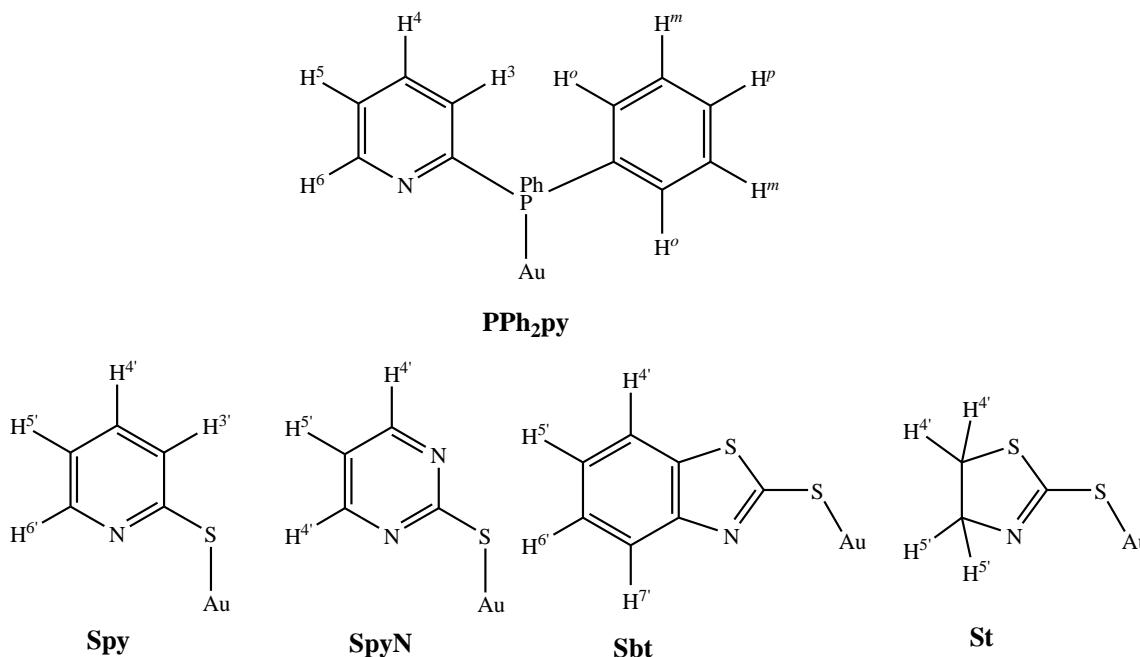
Figure 7. % Inhibition of complex **1c** and Auranofin on GR as well as their K_{inact} estimation. **1c** is more potent than auranofin in inhibition of GR.

4. Experimental

4.1. General procedures and materials

All reactions were carried out under an argon atmosphere using standard Schlenk techniques. NMR spectra (^1H and $^{31}\text{P}\{^1\text{H}\}$) were recorded on a Bruker Avance DPX 400 MHz instrument at 298 K. All chemical shifts are reported in ppm (part per million) relative to their corresponding external standards (SiMe_4 for ^1H (400 MHz) and 85% H_3PO_4 for ^{31}P (162 MHz)) and all the coupling constants (J values) are given in Hz. The microanalyses were performed using a vario EL CHNS elemental analyzer. 2-(Diphenylphosphino)pyridine (PPh₂py), pyridine-2-thiol (HSp_y), pyrimidine-2-thiol (HSp_yN), benzothiazole-2-thiol (HSbt) and 2-thiazoline-2-thiol (HSt) were purchased from Aldrich or Acros. Also, all solvents were purchased from Aldrich and used

without further purification. Complex [(PPh₂py)AuCl], **A**, was prepared as reported in literature.³⁷ The chemical shift assignments are based on the following NMR labeling for the ligands as are shown in Scheme 2. Additional data for **A**: NMR data in CDCl₃: δ (¹H) 8.79 (d, ³J_{HH} = 4.7 Hz, 1H, H⁶), 7.98 (t, ³J_{HH} = 7.9 Hz, 1H, H³), 7.80 (tdd, ³J_{HH} = 7.9, ⁴J_{HH} = 1.8 Hz, ⁴J_{PH} = 3.7 Hz, 1H, H⁴), 7.69 (ddd, ³J_{HH} = 7.2, ⁴J_{HH} = 1.4 Hz, ³J_{PH} = 13.4 Hz, 4H, H^o), 7.43-7.54 (m, 6H, H^m and H^p), 7.40 (td, ³J_{HH} = 7.8, ⁴J_{HH} = 1.6 Hz, 1H, H⁵) ppm. δ (³¹P{¹H}) 32.2 (s, 1P) ppm.



Scheme 2. Numerical Scheme for ¹H NMR assignment.

4.2. Synthesis of complexes

4.2.1. [(PPh₂py)Au(κ^1 -S-Spy)], **1a**.

Complex **A** (100 mg, 0.202mmol) was added to an ethanolic solution of potassium pyridine-2-thiolate ligand (KC₅H₄NS) under inert atmosphere condition [KC₅H₄NS prepared by dissolving of KOH (15 mg, 0.262mmol, 1.3eq) in 10 mL of absolute ethanol and was treated with pyridine-2-thiol (23 mg, 0.202mmol) and stirred for 15 min]. Yellow solution was formed and after stirring for 2 h at room temperature and the solvent was removed under reduced pressure and the residue was extracted with CH₂Cl₂ (10 mL). The obtained colorless solution was filtered through celite and the filtrate was concentrated to a small volume (~ 1 mL) under vacuum, and

diethyl ether (5 mL) was added to give **1a** as a pale yellow solid, which was filtered and washed with diethyl ether (3 × 3 mL) and dried. Yield: 94 mg, 82%. Elem. Anal. Calcd. for C₂₂H₁₈AuN₂PS (570.40); C, 46.32; H, 3.18; N, 4.91. Found: C, 46.39; H, 3.21; N, 4.97. NMR data in CDCl₃: δ (¹H) 8.79 (d, ³J_{HH} = 4.6 Hz, 1H, H⁶), 8.28 (d, ³J_{HH} = 5.4 Hz, 1H, H⁶), 8.15 (t, ³J_{HH} = 7.7 Hz, 1H, H³), 7.76-7.82 (m, 5H, H⁴ and H^o), 7.44-7.52 (m, 7H, H⁴, H^m and H^p), 7.37 (td, ³J_{HH} = 7.7, ⁴J_{HH} = 1.4 Hz, 1H, H⁵), 7.31 (td, ³J_{HH} = 7.6, ⁴J_{HH} = 1.8 Hz, 1H, H³), 6.87 (td, ³J_{HH} = 7.2, ⁴J_{HH} = 1.1 Hz, 1H, H⁵) ppm. δ (³¹P{¹H}) 36.1 (s, 1P) ppm.

The other new complexes were made similarly using **A** and the appropriate thiol ligands.

4.2.2. [(PPh₂py)Au(κ¹-S-SpyN)], **1b**.

Yield: 86 mg, 74%. Elem. Anal. Calcd. for C₂₁H₁₇AuN₃PS (571.39): C, 44.14; H, 3.00; N, 7.35. Found: C, 44.23; H, 3.04; N, 7.42. NMR data in CDCl₃: δ (¹H) 8.83 (d, ³J_{HH} = 4.8 Hz, 1H, H⁶), 8.41 (d, ³J_{HH} = 4.9 Hz, 2H, H⁴), 8.24 (td, ³J_{HH} = 8.1 Hz, ⁴J_{HH} = 1.0 Hz, 1H, H³), 7.87 (ddd, ³J_{HH} = 7.9, ⁴J_{HH} = 1.1 Hz, ³J_{PH} = 14.0 Hz, 4H, H^o), 7.83 (tdd, ³J_{HH} = 7.7, ⁴J_{HH} = 1.9 Hz, ⁴J_{PH} = 3.6 Hz, 1H, H⁴), 7.47-7.56 (m, 6H, H^m and H^p), 7.41 (m, 1H, H⁵), 6.88 (t, ³J_{HH} = 4.9 Hz, 1H, H⁵) ppm. δ (³¹P{¹H}) 37.1 (s, 1P) ppm.

4.2.3. [(PPh₂py)Au(κ¹-S-Sbt)], **1c**.

Yield: 100 mg, 79%. Elem. Anal. Calcd. for C₂₄H₁₈AuN₂PS₂ (626.49): C, 46.01; H, 2.90; N, 4.47. Found: C, 45.95; H, 2.98; N, 4.59. NMR data in CDCl₃: δ (¹H) 8.82 (d, ³J_{HH} = 4.6 Hz, 1H, H⁶), 8.10 (t, ³J_{HH} = 7.7 Hz, 1H, H³), 7.78-7.85 (m, 5H, H⁴ and H^o), 7.73 (d, ³J_{HH} = 7.8 Hz, 1H, H⁷), 7.59 (d, ³J_{HH} = 7.9 Hz, 1H, H⁴), 7.47-7.55 (m, 6H, H^m and H^p), 7.42 (m, 1H, H⁵), 7.32 (t, ³J_{HH} = 7.8 Hz, 1H, H⁶), 7.18 (t, ³J_{HH} = 7.8 Hz, 1H, H⁵) ppm. δ (³¹P{¹H}) 36.7 (s, 1P) ppm.

4.2.4. [(PPh₂py)Au(κ¹-S-St)], **1d**.

Yield: 106 mg, 91%. Elem. Anal. Calcd. for C₂₀H₁₈AuN₂PS₂ (578.44): C, 41.53; H, 3.14; N, 4.84. Found: C, 41.65; H, 3.20; N, 4.91. NMR data in CDCl₃: δ (¹H) 8.79 (d, ³J_{HH} = 4.6 Hz, 1H, H⁶), 8.08 (t, ³J_{HH} = 7.8 Hz, 1H, H³), 7.74-7.83 (m, 5H, H⁴ and H^o), 7.44-7.53 (m, 6H, H^m and H^p), 7.39 (m, 1H, H⁵), 4.30 (t, ³J_{HH} = 8.0 Hz, 2H, H⁵), 3.41 (t, ³J_{HH} = 8.0 Hz, 2H, H⁴) ppm. δ (³¹P{¹H}) 36.6 (s, 1P) ppm.

4.3. Crystal structure determination and refinement

The X-ray diffraction measurement was carried out on STOE IPDS2T diffractometer with graphite-monochromated Mo K α radiation. The single crystals suitable for X-ray analysis were obtained from CH₂Cl₂/*n*-hexane solution (at room temperature) and mounted on a glass fiber and used for data collection. Cell constants and an orientation matrix for data collection were obtained by least-square refinement of the diffraction data for **1b** and **1d**. Diffraction data were collected in a series of ω scans in 1° oscillations and integrated using the Stoe X-AREA software package.⁴² Numerical absorption correction was applied using X-Red32 software. The structure was solved by direct methods and subsequent difference Fourier maps and then refined on F2 by a full-matrix least-squares procedure using anisotropic displacement parameters. Atomic factors are from the International Tables for X-ray Crystallography. All non-hydrogen atoms were refined with anisotropic displacement parameters. Hydrogen atoms were placed in ideal positions and refined as riding atoms with relative isotropic displacement parameters. All refinements were performed using the X-STEP32, SHELXL-2014 and WinGX-2013.3 programs.⁴³⁻⁴⁷ Crystallographic data for the structural analysis has been deposited with the Cambridge Crystallographic Data Centre, No. CCDC-1574994 (for **1b**) and CCDC-1574995 (for **1d**).

4.4. Biological Assay

4.4.1. Cell Lines and Cell Culture

Human cancer cell lines, MCF-7 (breast cancer), SKOV3 (ovarian cancer), SW1116 (colon cancer), Hela (cervical cancer) and A549 (non-small cell lung cancer) were purchased from National Cell Bank of Iran (NCBI, Pasteur Institute, Tehran, Iran). All cancer cells were cultured in RPMI 1640 (BioIdea), except MCF-7 which were cultured in DMEM medium supplemented with 10% fetal bovine serum (FBS; Gibco) and 1% penicillin-streptomycin and were incubated at 37 °C in humidified CO₂ incubator. MCF-12A was cultured in medium containing DMEM/ Ham's F12 in the presence of 2.5% horse serum and supplemented with epidermal growth factor, hydrocortisone, bovine insulin, cholera toxin, and antibiotic/antimycotic. 3-(4,5-dimethylthiazolyl)-2,5-diphenyl-tetrazolium bromide (MTT) assay was applied for assessing the cytotoxic activities of **A** and **1a-d** as previously described.⁴⁸⁻⁵⁰ Briefly, the cells were trypsinized and plated in 96-well microplates per well. The cells were then treated with different concentrations of the

gold complexes (1 to 100 μM) in triplicate manner. Following 48 h incubation at 37 $^{\circ}\text{C}$ in humidified CO_2 incubator, in order to dissolve the formazan crystals, the media were completely discarded and replaced with 150 μL of 0.5 mg/mL MTT solution and incubated for 3-4 h at 37 $^{\circ}\text{C}$. The media containing MTT was then replaced with 150 μL of DMSO. The plate were incubated for more 30 min at 37 $^{\circ}\text{C}$ in the dark. The absorbance of each well was obtained at 490 nm using a microplate ELISA reader. The data were analyzed using Excel 2013 and CurveExpert 1.4 and the concentration with 50% inhibitory effect was reported as IC_{50} of each compound. Each experiment was separately repeated three times. Data are presented as mean \pm SD.

4.4.2. Apoptosis detection

PE Annexin V Apoptosis Detection Kit I from BD Biosciences was used for detection of apoptosis. To do this, 50000 cells was cultured in complete culture media in a 24-well culture plate. The cells were then treated with different concentrations of complex **1b** (2.5, 5 and 10 μM) and incubated at 37 $^{\circ}\text{C}$ with 5% CO_2 for 48 hours. An untreated sample with equivalent DMSO concentration was also used as the control. The cells were then harvested, washed with the cold PBS 1X and re-suspended in 1X Binding Buffer. 1×10^5 of the cells in 50 μl Binding Buffer were transferred to the tubes, stained with 2 μl of FITC-conjugated Annexin V as well as 2 μl of 7-AAD (7-Aminoactinomycin D) solution and incubated for 15 min at room temperature in the dark. 300 μl of 1X Binding Buffer was added to each tube and analyzed immediately by four-color FACSCalibur flow cytometer (BD Bioscience, USA). At least 50000 cells were acquired. The data were analyzed by flowJo software packages.

4.4.3. Trx1/insulin assay

130 nM TrxR1 was reduced in 200 μM NADPH in Tris-EDTA (TE) buffer and incubated at room temperature with increasing concentrations (0.125 μM , 0.25 μM , 0.5 μM , 1 μM , 2 μM and 4 μM) of Auranofin and the gold(I) complexes (**A** and **1a-d**) for different time points (5, 30, 60 and 90 minutes). Aliquots were removed and added to a mixture containing 25 μM Trx1, 160 μM insulin and 200 μM NADPH in TE buffer. NADPH consumption at 30 $^{\circ}\text{C}$ was measured at 340 nm using the VersaMax microplate reader. The percentage of inactivation compared to DMSO control was plotted against time using GraphPad Prism 5.0a (GraphPad software, Inc.). The resulting slopes (k_{obs}), were plotted against the inhibitor concentrations resulting in K_{inact} .

4.4.4. Trx2/insulin assay

130 nM TrxR2 was reduced in 200 μ M NADPH in Tris-EDTA (TE) buffer and incubated at room temperature with Auranofin in 1 μ M and the gold(I) complexes (**A** and **1a-d**) in 20 μ M for different time points (5, 30, 60 and 90 minutes). Aliquots were removed and added to a mixture containing 25 μ M Trx2, 160 μ M insulin and 200 μ M NADPH in TE buffer. NADPH consumption at 30°C was measured at 340 nm using the VersaMax microplate reader.

4.4.5. Glutathione reductase assay

160 nM GR was reduced by 250 μ M NADPH in 0.1 M potassium phosphate buffer, pH 7.0 containing 1 mM EDTA. Auranofin and the gold(I) complexes (**A** and **1a-d**) was added at increasing concentrations (0.125 μ M, 0.25 μ M, 0.5 μ M, 1 μ M, 2 μ M and 4 μ M) and incubated with the enzyme at room temperature. At various time points (5, 30, 60 and 90 minutes), aliquots were removed and GR activity was measured in the presence of 100 μ M NADPH, 1 mM glutathione disulfide (GSSG) and 1 mM EDTA in potassium phosphate buffer at 340 nm using the VersaMax microplate reader.

Acknowledgements

M.H.B. gratefully acknowledges the financial support through the startup funds from the University of Arkansas. The Institute for Advanced Studies in Basic Sciences (IASBS) Research Council, the Department of Medicinal Chemistry, School of Pharmacy, Ahvaz Jundishapur University of Medical Sciences (GP95120 and B-9550) and the Iran National Science Foundation (Grant no 96007334) are also gratefully acknowledged. H.R.S. wish to acknowledge IASBS for their sabbatical leave at University of Arkansas. Prof. Elias Arnér and Belen Espinosa are gratefully acknowledged for performing the cytosolic (TrxR1), mitochondrial (TrxR2) thioredoxin reductases and glutathione reductase (GR) tests.

References

1. S. Nobili, E. Mini, I. Landini, C. Gabbiani, A. Casini and L. Messori, *Med. Res. Rev.*, 2010, **30**, 550-580.
2. I. Romero-Canelón and P. J. Sadler, *Inorg. Chem.*, 2013, **52**, 12276-12291.

3. C. Nardon, G. Boscutti and D. Fregona, *Anticancer Res.*, 2014, **34**, 487-492.
4. S. J. Berners-Price and P. J. Barnard, *Ligand Design in Medicinal Inorganic Chemistry*, 2014, 227-256.
5. I. Ott, *Coord. Chem. Rev.*, 2009, **253**, 1670-1681.
6. S. J. Berners-Price and A. Filipovska, *Metallomics*, 2011, **3**, 863-873.
7. G. Gasser and N. Metzler-Nolte, *Curr. Opin. Chem. Bio.*, 2012, **16**, 84-91.
8. B. Bertrand and A. Casini, *Dalton Trans.*, 2014, **43**, 4209-4219.
9. S. Medici, M. Peana, V. M. Nurchi, J. I. Lachowicz, G. Crisponi and M. A. Zoroddu, *Coord. Chem. Rev.*, 2015, **284**, 329-350.
10. K. P. Bhabak, B. J. Bhuyan and G. Mugesh, *Dalton Trans.*, 2011, **40**, 2099-2111.
11. M. J. McKeage, L. Maharaj and S. J. Berners-Price, *Coord. Chem. Rev.*, 2002, **232**, 127-135.
12. A. Bindoli, M. P. Rigobello, G. Scutari, C. Gabbiani, A. Casini and L. Messori, *Coord. Chem. Rev.*, 2009, **253**, 1692-1707.
13. P. J. Barnard and S. J. Berners-Price, *Coord. Chem. Rev.*, 2007, **251**, 1889-1902.
14. A. Gutiérrez, L. Gracia-Fleta, I. Marzo, C. Cativiela, A. Laguna and M. C. Gimeno, *Dalton Trans.*, 2014, **43**, 17054-17066.
15. J. Carlos Lima and L. Rodriguez, *Anti-Cancer Agents in Med. Chem.*, 2011, **11**, 921-928.
16. A. Gutiérrez, I. Marzo, C. Cativiela, A. Laguna and M. C. Gimeno, *Chem. Eur. J.*, 2015, **21**, 11088-11095.
17. E. García-Moreno, S. Gascón, E. Atrián-Blasco, M. J. Rodríguez-Yoldi, E. Cerrada and M. Laguna, *Eur. J. Med. Chem.*, 2014, **79**, 164-172.
18. S. Miranda, E. Vergara, F. Mohr, D. de Vos, E. Cerrada, A. Mendía and M. Laguna, *Inorg. Chem.*, 2008, **47**, 5641-5648.
19. E. Vergara, E. Cerrada, C. Clavel, A. Casini and M. Laguna, *Dalton Trans.*, 2011, **40**, 10927-10935.
20. E. Vergara, A. Casini, F. Sorrentino, O. Zava, E. Cerrada, M. P. Rigobello, A. Bindoli, M. Laguna and P. J. Dyson, *ChemMedChem*, 2010, **5**, 96-102.
21. F. K. Keter, I. A. Guzei, M. Nell, W. E. v. Zyl and J. Darkwa, *Inorg. Chem.*, 2014, **53**, 2058-2067.
22. P. J. Sadler and R. E. Sue, *Metal-Based Drugs*, 1994, **1**, 107-144.

- 1
2
3
4
5
6
7
8
9
10
11
12
13
14
15
16
17
18
19
20
21
22
23
24
25
26
27
28
29
30
31
32
33
34
35
36
37
38
39
40
41
42
43
44
45
46
47
48
49
50
51
52
53
54
55
56
57
58
59
60
23. C. F. Shaw, *Chem. Rev.*, 1999, **99**, 2589-2600.
24. C.-M. Che and R. W.-Y. Sun, *Chem. Commun.*, 2011, **47**, 9554-9560.
25. E. R. T. Tiekink, *Crit. Rev. Oncol. Hemat.*, 2002, **42**, 225-248.
26. Z.-Z. Zhang and H. Cheng, *Coord. Chem. Rev.*, 1996, **147**, 1-39.
27. M. C. Gimeno and A. Laguna, *Chem. Soc. Rev.*, 2008, **37**, 1952-1966.
28. S. Jamali, R. Ghazfar, E. Lalinde, Z. Jamshidi, H. Samouei, H. R. Shahsavari, M. T. Moreno, E. Escudero-Adán, J. Benet-Buchholz and D. Milic, *Dalton Trans.*, 2014, **43**, 1105-1116.
29. L. Hao, M. A. Mansour, R. J. Lachicotte, H. J. Gysling and R. Eisenberg, *Inorg. Chem.*, 2000, **39**, 5520-5529.
30. M. J. Calhorda, C. Ceamanos, O. Crespo, M. C. n. Gimeno, A. Laguna, C. Larraz, P. D. Vaz and M. D. Villacampa, *Inorg. Chem.*, 2010, **49**, 8255-8269.
31. S. Jamali, Z. Mazloomi, S. M. Nabavizadeh, D. Milić, R. Kia and M. Rashidi, *Inorg. Chem.*, 2010, **49**, 2721-2726.
32. M. Rashidi, M. C. Jennings and R. J. Puddephatt, *Organometallics*, 2003, **22**, 2612-2618.
33. P. Espinet and K. Soulantica, *Coord. Chem. Rev.*, 1999, **193**, 499-556.
34. C. Khin, A. S. K. Hashmi and F. Rominger, *Eur. J. Inorg. Chem.*, 2010, **2010**, 1063-1069.
35. V. J. Catalano, J. M. López-de-Luzuriaga, M. Monge, M. E. Olmos and D. Pascual, *Dalton Trans.*, 2014, **43**, 16486-16497.
36. A. Gutiérrez, C. Cativiela, A. Laguna and M. C. Gimeno, *Dalton Trans.*, 2016, **45**, 13483-13490.
37. C. Khin, A. S. K. Hashmi and F. Rominger, *Eur. J. Inorg. Chem.*, 2010, **2010**, 1063-1069.
38. M.-C. Brandys, M. C. Jennings and R. J. Puddephatt, *J. Chem. Soc., Dalton Trans.*, 2000, 4601-4606.
39. J. D. Wilton-Ely, A. Schier, N. W. Mitzel and H. Schmidbaur, *J. Chem. Soc., Dalton Trans.*, 2001, 1058-1062.
40. F. M. Monzittu, V. Fernández-Moreira, V. Lippolis, M. Arca, A. Laguna and M. C. Gimeno, *Dalton Trans.*, 2014, **43**, 6212-6220.
41. W. C. Stafford, X. Peng, M. H. Olofsson, X. Zhang, D. K. Luci, L. Lu, Q. Cheng, L. Trésaugues, T. S. Dexheimer, N. P. Coussens, M. Augsten, H.-S. M. Ahlén, O. Orwar, A.

- 1
2
3 Östman, S. Stone-Elander, D. J. Maloney, A. Jadhav, A. Simeonov, S. Linder and E. S. J.
4 Arnér, *Sci. Transl. Med.*, 2018, **10**, eaaf7444.
5
6 42. Stoe & Cie, X–AREA: Program for the Acquisition and Analysis of Data, Version 1.30;
7 Stoe & Cie GmbH: Darmsatadt, Germany, 2005.
8
9 43. M. N. Burnett and C. K. Johnson, ORTEP-III Report ORNL-6895. Oak Ridge National
10 Laboratory, Tennessee, USA 1996.
11
12 44. P. Coppens, L. Leiserowitz and D. Rabinovich, *Acta Crystallogr.*, 1965, **18**, 1035-1038.
13
14 45. L. J. Farrugia, *J. Appl. Cryst.*, 1999, **32**, 837-838.
15
16 46. C. F. Macrae, P. R. Edgington, P. McCabe, E. Pidcock, G. P. Shields, R. Taylor, M. Towler
17 and J. van der Streek, *J. Appl. Cryst.*, 2006, **39**, 453-457.
18
19 47. G. M. Sheldrick, *Acta Crystallogr., Sect. A*, 2008, **64**, 112-122.
20
21 48. M. Fereidoonzezhad, B. Kaboudin, T. Mirzaee, R. Babadi Aghakhanpour, M. Golbon
22 Haghghi, Z. Faghiih, Z. Faghiih, Z. Ahmadipour, B. Notash and H. R. Shahsavari,
23 *Organometallics*, 2017, **36**, 1707–1717.
24
25 49. M. Fereidoonzezhad, M. Niazi, Z. Ahmadipour, T. Mirzaee, Z. Faghiih, Z. Faghiih and H.
26 R. Shahsavari, *Eur. J. Inorg. Chem.*, 2017, 2247–2254.
27
28 50. M. Fereidoonzezhad, M. Niazi, M. Shahmohammadi Beni, S. Mohammadi, Z. Faghiih, Z.
29 Faghiih and H. R. Shahsavari, *ChemMedChem*, 2017, **12**, 456-465.
30
31
32
33
34
35
36
37
38
39
40
41
42
43
44
45
46
47
48
49
50
51
52
53
54
55
56
57
58
59
60

Table of Contents Entry

Synthesis and biological evaluation of thiolate gold(I) complexes as thioredoxin reductases (TrxRs) and glutathione reductase (GR) inhibitors

Gold(I) complexes with 2-(diphenylphosphino)pyridine and thiolate ligands are prepared and studied for their antiproliferative effects in tumor and normal cells *in vitro*. The complexes are also revealed to efficiently inhibit the thioredoxin reductases (TrxR) and glutathione reductase (GR).

